

Bridge Sampling Diagnostics

Giorgio Micaletto^{*1} and Aki Vehtari²

¹*Bocconi University, Italy*

²*ELLIS Institute Finland; Department of Computer Science, Aalto University, Finland*

Abstract. In Bayesian statistics, the marginal likelihood is used for model selection and averaging, yet it is often challenging to compute accurately for complex models. Approaches such as bridge sampling, while effective, may suffer from issues of high variability of the estimates. We present how to estimate Monte Carlo standard error (MCSE) for bridge sampling, and how to diagnose the reliability of MCSE estimates using Pareto- \hat{k} and block reshuffling diagnostics without the need to repeatedly re-run full posterior inference. We demonstrate the behavior with increasingly more difficult simulated posteriors and many real posteriors from the posteriordb database.

Keywords: Marginal Likelihood, Normalizing Constant, Monte Carlo Standard Error

1 Introduction

Marginal likelihoods (model evidences) are often used for Bayesian model comparison (e.g. Bayes factors), model averaging, and calibrating prior and model components. At the same time, it is well understood that evidence-based workflows can be fragile in practice: marginal likelihood estimates can be extremely sensitive to prior specification and to numerical error, with different estimators' behavior varying significantly across models and data. We do not advocate marginal likelihood as a universal model selection tool; rather, our goal is to reduce wasted computation and failure-by-silence by providing practical diagnostics for assessing the *Monte Carlo reliability* of evidence estimates computed from a finite number of posterior draws (see, e.g., Friel and Wyse, 2012; Fourment et al., 2019 for broader reviews and cautions).

Let \mathcal{M} denote a Bayesian model with parameter vector $\theta \in \Theta \subseteq \mathbb{R}^p$ (where $p := \dim(\theta)$) and observed data vector $\mathbf{y} = (y_1, \dots, y_n)^\top \in \mathbb{R}^n$.

$$p(\mathbf{y} \mid \mathcal{M}) = \int_{\Theta} p(\mathbf{y} \mid \theta, \mathcal{M}) p(\theta \mid \mathcal{M}) d\theta, \quad (1)$$

which is generally intractable for realistic models and thus requires approximation. Among sampling-based methods, bridge sampling has a long history starting from the acceptance-ratio ideas of Bennett (1976) and the general formulation of Meng and Wong (1996), with connections to importance sampling and path sampling emphasized by Gelman and Meng (1998). In modern Bayesian workflows bridge sampling has become a practical default, in part due to robust implementations and tutorials (e.g., Gronau et al., 2017, 2020a).

Despite its practical appeal, bridge sampling is not “automatic” in the sense that a single run would always yield a numerically reliable estimate at typical posterior sample sizes; the estimator is a ratio of empirical averages whose stability is governed by overlap between the posterior and the proposal distribution and by the behavior of rare, extreme terms. In high-dimensional or strongly non-Gaussian posteriors, the distribution of the summands can exhibit severe pre-asymptotic behavior, so that a small number of atypical draws may dominate the estimate long before the asymptotic \sqrt{S} regime becomes a useful approximation. Re-running full posterior inference to assess Monte Carlo variability is often

^{*}The majority of this work was completed while the author was working at Aalto University.

Bridge Sampling Diagnostics

computationally expensive, and practitioners therefore greatly benefit from diagnostics that can be computed from existing posterior draws and likelihood evaluations.

We develop a diagnostic workflow for bridge sampling that aims to answer a simple practical question: *given the posterior draws already available, should we trust the reported marginal likelihood estimate and its Monte Carlo uncertainty?* Concretely, we make three contributions:

- (i) We derive a closed-form Monte Carlo standard error (MCSE) estimator for the bridge sampling estimate (and its logarithm), accounting for autocorrelation in MCMC draws via effective sample size adjustments.
- (ii) We adapt Pareto tail-index diagnostics (Pareto- \widehat{k}) to the bridge sampling setting to flag finite-sample instability in the numerator and denominator contributions, complementing the MCSE.
- (iii) We introduce a block reshuffling diagnostic, a resampling procedure related to bootstrapping, demonstrating how this tool captures the skewness and non-normality of the estimator's sampling distribution in finite samples, properties that the standard CLT-based MCSE cannot detect.

We demonstrate the behavior of these diagnostics using increasingly difficult simulated posteriors, and across a broad suite of real posteriors from the `posteriorsdb` database.

2 Bridge Sampling

Write the unnormalized posterior density as

$$\tilde{\pi}(\boldsymbol{\theta}) := p(\mathbf{y} \mid \boldsymbol{\theta}, \mathcal{M}) p(\boldsymbol{\theta} \mid \mathcal{M}), \quad \pi(\boldsymbol{\theta}) = \frac{\tilde{\pi}(\boldsymbol{\theta})}{Z}, \quad Z := p(\mathbf{y} \mid \mathcal{M}) = \int_{\Theta} \tilde{\pi}(\boldsymbol{\theta}) d\boldsymbol{\theta}.$$

Bridge sampling estimates the normalizing constant Z by introducing a *normalized* proposal density $g(\boldsymbol{\theta})$ (from which we can both sample and evaluate pointwise) whose support contains that of the posterior $\pi(\boldsymbol{\theta})$, together with a bridge function $h(\boldsymbol{\theta})$ (also denoted $\omega(\boldsymbol{\theta})$ in parts of the literature). Formally, $h(\boldsymbol{\theta})$ is a user-chosen auxiliary function defined on the common support of π and g such that

$$0 < \left| \int_{\Theta} h(\boldsymbol{\theta}) \pi(\boldsymbol{\theta}) g(\boldsymbol{\theta}) d\boldsymbol{\theta} \right| < \infty.$$

Provided this condition holds, $h(\boldsymbol{\theta})$ acts as an algebraic device satisfying the exact identity

$$Z = \frac{\mathbb{E}_g[\tilde{\pi}(\boldsymbol{\theta}) h(\boldsymbol{\theta})]}{\mathbb{E}_\pi[g(\boldsymbol{\theta}) h(\boldsymbol{\theta})]}, \tag{2}$$

where

$$\mathbb{E}_g[f(\boldsymbol{\theta})] := \int_{\Theta} f(\boldsymbol{\theta}) g(\boldsymbol{\theta}) d\boldsymbol{\theta}$$

and

$$\mathbb{E}_\pi[f(\boldsymbol{\theta})] := \int_{\Theta} f(\boldsymbol{\theta}) \pi(\boldsymbol{\theta}) d\boldsymbol{\theta}.$$

Hence, h defines the resulting Monte Carlo estimator and strongly affects its variance through how it reweights regions where π and g overlap, with many familiar estimators arising as special cases of bridge sampling via particular choices of h (e.g., importance sampling and reciprocal-importance/harmonic-mean-type estimators).

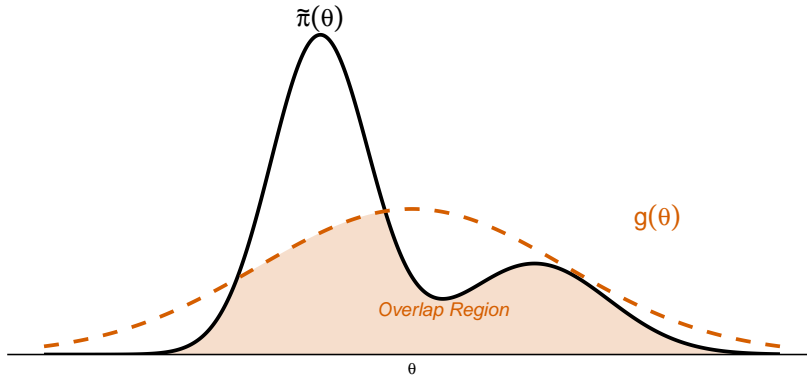


Figure 1. Intuition of the bridge sampling estimator. It relies on the ratio of the unnormalized posterior $\tilde{\pi}(\boldsymbol{\theta})$ (solid line) and the proposal density $g(\boldsymbol{\theta})$ (dashed line), and its stability depends on the *overlap* (shaded region) between the two distributions.

Using the identity (2), we obtain the empirical estimator

$$\widehat{Z} = \widehat{p}(\mathbf{y} \mid \mathcal{M}) = \frac{\frac{1}{S_2} \sum_{i=1}^{S_2} \tilde{\pi}(\tilde{\boldsymbol{\theta}}_i) h(\tilde{\boldsymbol{\theta}}_i)}{\frac{1}{S_1} \sum_{j=1}^{S_1} h(\boldsymbol{\theta}_j^*) g(\boldsymbol{\theta}_j^*)}, \quad (3)$$

where $\boldsymbol{\theta}_j^* \sim \pi(\boldsymbol{\theta})$ are (typically MCMC) S_1 posterior draws and $\tilde{\boldsymbol{\theta}}_i \sim g(\boldsymbol{\theta})$ are S_2 independent proposal draws.

The practical performance of bridge sampling is governed by overlap between $\pi(\boldsymbol{\theta})$ and $g(\boldsymbol{\theta})$ (see Figure 1), which is frequently chosen as a multivariate normal distribution in the unconstrained parameter space, with mean and covariance estimated from posterior draws (see, e.g., Gronau et al., 2017, 2020a for the standard workflow). Because proposal fitting from posterior draws can introduce bias and/or lead to over-optimistic stability assessments if the same draws are reused, implementations often split posterior draws into subsets (one subset to fit g , one subset to estimate Z), trading reduced bias for increased Monte Carlo variability (Overstall and Forster, 2010; Wong et al., 2020). For a comprehensive tutorial and step-by-step implementation details, we refer the reader to Gronau et al. (2017).

As some models may present strongly non-Gaussian or multimodal posteriors, leading to poor overlap with normal proposals, a complementary line of work focuses on improving overlap by transforming (warping) the target to match more closely a tractable reference distribution (see, e.g., warp bridge sampling (Meng and Schilling, 2002; Gronau et al., 2020b) and Warp-U-style transformations for multimodal targets (Wang et al., 2022)). Our focus is not to introduce new proposals or warps, but rather to provide diagnostics that indicate when the default workflow is already reliable and when additional computational investment (more posterior draws, better proposals/warps, or alternative evidence estimators) is warranted.

A widely used (near-optimal) choice of $h(\boldsymbol{\theta})$ is the one proposed by Meng and Wong (1996),

$$h(\boldsymbol{\theta}) \propto \frac{1}{s_1 \tilde{\pi}(\boldsymbol{\theta}) + s_2 Z g(\boldsymbol{\theta})}, \quad (4)$$

where

$$s_1 := \frac{S_1}{S_1 + S_2} \quad \text{and} \quad s_2 := \frac{S_2}{S_1 + S_2}.$$

Bridge Sampling Diagnostics

More generally, while the asymptotically optimal bridge function under independence is proportional to the reciprocal of a mixture of the two (unnormalized) densities (Bennett, 1976; Meng and Wong, 1996), because this optimal form depends on the unknown Z , it is implemented in practice via the fixed-point iteration in (5).

Defining

$$l_{1,j} := \frac{\tilde{\pi}(\boldsymbol{\theta}_j^*)}{g(\boldsymbol{\theta}_j^*)}, \quad l_{2,i} := \frac{\tilde{\pi}(\tilde{\boldsymbol{\theta}}_i)}{g(\tilde{\boldsymbol{\theta}}_i)},$$

the standard update takes the form

$$\widehat{Z}^{(t+1)} = \frac{\frac{1}{S_2} \sum_{i=1}^{S_2} \frac{l_{2,i}}{s_1 l_{2,i} + s_2 \widehat{Z}^{(t)}}}{\frac{1}{S_1} \sum_{j=1}^{S_1} \frac{1}{s_1 l_{1,j} + s_2 \widehat{Z}^{(t)}}}, \quad \text{with } \widehat{Z}^{(0)} = 1, \quad (5)$$

iterating until the update is smaller than a tolerance (or until a maximum number of iterations is reached).

Bridge sampling is typically less sensitive than plain importance sampling to modest tail mismatch because the update in (5) involves bounded ratios (see, e.g., Gronau et al., 2017). However, boundedness alone does not guarantee stable finite-sample behavior: when overlap is poor, the effective range of the summands can be so wide that rare extreme realizations dominate at practical sample sizes S_1 and S_2 . The remainder develops MCSE estimation and complementary diagnostics aimed at detecting exactly these pre-asymptotic failure modes without requiring repeated posterior inference.

3 Monte Carlo Standard Error

As the first step to assess the precision of the bridge sampling estimate, we propose to compute Monte Carlo standard error (MCSE). The estimator \widehat{Z} given in Equation (3) is a ratio of two sample means: $\widehat{Z} = \bar{N}/\bar{D}$, with

$$\begin{aligned} \bar{N} &= \frac{1}{S_2} \sum_{i=1}^{S_2} N_i, \quad \text{where } N_i := \tilde{\pi}(\tilde{\boldsymbol{\theta}}_i) h(\tilde{\boldsymbol{\theta}}_i), \\ \bar{D} &= \frac{1}{S_1} \sum_{j=1}^{S_1} D_j, \quad \text{where } D_j := h(\boldsymbol{\theta}_j^*) g(\boldsymbol{\theta}_j^*). \end{aligned} \quad (6)$$

To compute the variance of \widehat{Z} , we use the delta method, thus, the variance estimate is:

$$\text{Var}(\widehat{Z}) \approx \frac{1}{S_1} \left(\frac{\bar{N}}{\bar{D}} \right)^2 \left(\frac{\text{Var}(\bar{N})}{\bar{N}^2} + \frac{\text{Var}(\bar{D})}{\bar{D}^2} - 2 \frac{\text{Cov}(\bar{N}, \bar{D})}{\bar{N} \bar{D}} \right), \quad (7)$$

assuming that $S_1 = S_2$. As \bar{N} and \bar{D} are sample means, their variances and covariance are:

$$\text{Var}(\bar{N}) := \frac{\text{Var}(N_i)}{S_2}, \quad \text{Var}(\bar{D}) := \frac{\text{Var}(D_j)}{S_1}, \quad \text{Cov}(\bar{N}, \bar{D}) := \frac{\text{Cov}(N_i, D_j)}{S_1}.$$

The draws $\tilde{\boldsymbol{\theta}}_i$ and $\boldsymbol{\theta}_j^*$ are independent, and thus $\text{Cov}(\bar{N}, \bar{D}) = 0$. Substituting back, we get

$$\text{Var}(\widehat{Z}) \approx \left(\frac{\bar{N}}{\bar{D}} \right)^2 \left(\frac{\text{Var}(N_i)}{S_2 \bar{N}^2} + \frac{\text{Var}(D_j)}{S_1 \bar{D}^2} \right). \quad (8)$$

If θ_j^* are drawn using MCMC, terms D_j may also have significant autocorrelation and estimate for $\text{Var}(\bar{D})$ should then take that into account. In the experiments we used MCMC effective sample size estimate by Vehtari et al. (2021). Finally

$$\text{MCSE}(\widehat{Z}) = \sqrt{\text{Var}(\widehat{Z})}. \quad (9)$$

To compute the MCSE of the logarithm of the marginal likelihood estimate, $\log \widehat{Z}$, we use the property of the log-normal distribution to get

$$\text{Var}(\log \widehat{Z}) = \log \left(1 + \frac{\text{Var}(\widehat{Z})}{\widehat{Z}^2} \right).$$

Then

$$\text{MCSE}(\log \widehat{Z}) = \sqrt{\text{Var}(\log \widehat{Z})}. \quad (10)$$

The MCSE quantifies the uncertainty in the estimated (log) marginal likelihood due to the finite number of draws S_1 and S_2 , conditional on the proposal and the final bridge function when the iteration ends. In cases when the proposal is very different from the posterior or when the iterative algorithm fails to converge, there can be additional variation. In Section 5, we present a block reshuffling approach which takes into account all the parts of the bridge sampling algorithm. However, based on the experiments reported in Section 6, the presented MCSE estimator alone is often sufficiently precise.

4 Pareto- \widehat{k} Diagnostic and Pre-asymptotic Stability

The stability of the bridge sampling estimator relies on the convergence of the sample means \bar{N} and \bar{D} . A property of the optimal bridge function $h(\theta)$ is that the terms are strictly bounded. Since $g(\cdot)$ and $\tilde{\pi}(\cdot)$ are non-negative, the update equation implies:

$$0 \leq N_i \leq \frac{1}{s_1}, \quad 0 \leq D_j \leq \frac{1}{s_2} \quad \text{a.s.} \quad (11)$$

Consequently, all moments of N_i and D_j are theoretically finite, and the central limit theorem (CLT) holds asymptotically. However, asymptotic finite variance is insufficient for reliability in practice, as the convergence of the MCSE estimator depends on the sample variance converging to the population variance. We identify a specific regime where this convergence is critically slow, rendering standard variance estimators unreliable.

Define the *pre-asymptotic regime* \mathcal{R}_{pre} as the set of posterior-proposal pairs (π, g) and sample sizes S_1 and S_2 , where the effective support of the bridge function is unexplored. Let $r(\theta) = \tilde{\pi}(\theta)/g(\theta)$ be the unnormalized importance ratio. We say that a bridge sampling estimation is in \mathcal{R}_{pre} if the proposal $g(\theta)$ fails to uniformly cover the typical set of $\pi(\theta)$, such that the distribution of the importance weights exhibits heavy-tailed behavior within the observable range of S_1 and S_2 . This occurs under two primary conditions:

- (i) *Tail Mismatch*: The target $\pi(\theta)$ has heavier tails than the proposal $g(\theta)$ (e.g., a Student- t posterior approximated by a Gaussian proposal); here, $r(\theta) \rightarrow \infty$ in the tails, and while N_i is bounded by $1/s_1$, the probability of sampling near this bound is negligible for realistic S_2 .

- (ii) *High-Dimensional Mismatch*: Even with matching tail types, if D is sufficiently large, the variance of the log-weights satisfies $\text{Var}_g[\log r(\boldsymbol{\theta})] \gg 1$. The distribution of $r(\boldsymbol{\theta})$ becomes approximately Log-Normal with high variance, indistinguishable from a heavy-tailed distribution in finite samples.

In \mathcal{R}_{pre} , the values of N_i and D_j follow a power-law distribution $\mathbb{P}[X > x] \propto x^{-1/k}$ before truncating at the theoretical bounds. Standard variance estimators fail here as they are sensitive to the unobserved frequency of events near the bounds (Vehtari et al., 2024).

We propose the Pareto- \widehat{k} diagnostic as a *necessary condition* for sample size sufficiency. We fit the generalized Pareto distribution to the upper tails of $\{N_i\}$ and $\{D_j\}$:

$$\widehat{k}_N = \widehat{k}(\{N_i\}), \quad \widehat{k}_D = \widehat{k}(\{D_j\}).$$

Following the convergence rate analysis of importance sampling ratios in Vehtari et al. (2024), we establish the following validity criteria based on the estimated tail index \widehat{k} :

- (i) *Finite variance regime* ($\widehat{k} \leq 0.5$): When the tail index $k \leq 0.5$, the underlying distribution has a finite variance. In this regime, the standard central limit theorem applies, and the Monte Carlo error decreases at the standard rate of $O(S^{-1/2})$. Consequently, the standard MCSE (Section 3) is reliable and correctly characterizes the uncertainty of the estimator.
- (ii) *Smoothing-indicated regime* ($0.5 < \widehat{k} \leq 0.7$): In this range, the weight distribution exhibits pre-asymptotic behavior consistent with infinite variance, meaning the standard central limit theorem does not hold. In standard importance sampling, this instability is effectively mitigated using Pareto Smoothed Importance Sampling (PSIS, Vehtari et al., 2024), however, in bridge sampling, the terms N_i and D_j are strictly bounded (Equation 11), and empirically we observe that the tail index estimator \widehat{k} is often positively biased in this setting, interpreting the distribution’s slow decay toward its bound as a heavy, unbounded tail. Thus, applying Pareto smoothing based on an overestimated \widehat{k} risks imputing values that violate these bounds or assigning excessive probability mass to the tails, thereby potentially biasing the marginal likelihood estimate. Consequently, we do *not* apply smoothing and retain the raw estimator, which, while usable, exhibits convergence rates slower than $O(S^{-1/2})$, rendering the MCSE a likely underestimate of the true uncertainty.
- (iii) *Failure warning* ($\widehat{k} > 0.7$): If $\widehat{k} > 0.7$, the estimator operates deeply in the pre-asymptotic regime. The effective sample size is insufficient to explore the typical set, and the estimate is dominated by rare events. In this context, the variance-based MCSE is unreliable, and the result should not be trusted without increasing the sample size or improving the proposal.

When $\widehat{k} > 0.5$, practitioners should exercise caution, and while values up to 0.7 may be tolerated if one accepts that the reported MCSE is optimistic, a high \widehat{k} suggests increasing the sample size S significantly or utilizing the Block Reshuffling diagnostic (Section 5) to obtain a more robust empirical estimate of the uncertainty.

5 Block Reshuffling Diagnostic

The analytic MCSE derived in Section 3 relies on the asymptotic normality guaranteed by the central limit theorem; however, as discussed in Section 4, in the pre-asymptotic regime the distribution of the bridge sampling estimator is often heavy-tailed or skewed, and in such cases, the symmetric confidence intervals implied by the standard error are often misleading. To diagnose these finite-sample pathologies, we

propose a block reshuffling diagnostic, which adapts the blocking strategy of the moving block bootstrap (Kunsch, 1989) to the specific workflow of bridge sampling, using permutations to assess stability.

Standard resampling methods assume independent and identically distributed data; however, as MCMC draws exhibit autocorrelation, simple reshuffling destroys the dependence structure necessary for valid inference; the block approach addresses this by resampling contiguous blocks of the Markov chain, thereby preserving the local dependence structure (autocorrelation) within blocks while treating the blocks themselves as exchangeable (Liu and Singh, 1992).

Our procedure operates as follows: let $\mathcal{S} = (\theta_1^*, \dots, \theta_S^*)$ denote the available posterior draws, we partition \mathcal{S} into B contiguous blocks; to generate a single replicate \widehat{Z}_r , we resample these blocks without replacement (i.e., permute the blocks) to form a new sequence of length S , and we then run the *full* bridge sampling procedure on this reshuffled sequence: the draws are split, the proposal $g(\theta)$ is fitted to the first half, and the iterative update (Equation 5) is run to convergence. This process is repeated R times to generate an empirical distribution of estimates $\{\widehat{Z}_r\}_{r=1}^R$.

By re-estimating the proposal density for each replicate, this procedure approximates the sampling distribution of the estimator conditional on the empirical distribution of the chain. Unlike the analytic MCSE, which is a moment-based estimator fixed to a single proposal fit, the reshuffling ensemble captures the sensitivity of the estimator to the specific partitioning of the posterior draws and the resulting proposal approximation.

We define the block reshuffling error as the standard deviation of the log-transformed replicates:

$$\widehat{\text{MCSE}}_{\text{BR}}(\log \widehat{Z}) := \sqrt{\frac{1}{R-1} \sum_{r=1}^R (\log \widehat{Z}_r - \overline{\log \widehat{Z}})^2}.$$

More importantly, the bootstrap distribution allows us to assess properties beyond variance, specifically skewness and tail behavior. As noted by Hall (1992), resampling methods are particularly effective at characterizing the shape of a sampling distribution, providing a more accurate picture of uncertainty than CLT-based approximations.

Lastly, we explicitly apply the Pareto- \widehat{k} diagnostic to the replicates $\{\widehat{Z}_r\}_{r=1}^R$ as a stability check. Empirically, this aggregate diagnostic proves more stable than monitoring the raw numerator and denominator contributions (Section 6). A high Pareto- \widehat{k} value in this setting serves as a supplementary warning signal, implying that the estimator’s instability is structural; in such cases, even repeated sampling from the posterior cannot guarantee reliability without further computational investment.

We caution, however, that while block reshuffling detects non-normality, it likely underestimates the total variance. Because the procedure permutes a fixed, finite realization of the Markov chain rather than sampling from the true posterior, it cannot fully capture the variation that would arise from independent MCMC runs (Gelman and Rubin, 1992). Consequently, $\widehat{\text{MCSE}}_{\text{BR}}$ should be viewed as a diagnostic lower bound: if the reshuffling error is large or the distribution is skewed, the estimate is certainly unstable; however, a small reshuffling error does not guarantee accuracy if the original chain failed to explore the typical set.

6 Experimental Results

This section presents the empirical evaluation of the bridge sampling method, along with the proposed diagnostics. Our analysis focuses primarily on the precision (variability) of the estimates rather than systematic bias, as we utilize the standard bridge sampling estimator without bias-inducing modifications (even in the pre-asymptotic regime, see Section 4), which implies that the estimator remains consistent

and asymptotically unbiased. In the finite-sample regime, errors are driven by variance and skewness rather than systematic shift; thus, assessing the reliability of the MCSE is equivalent to assessing the root mean square error (RMSE).

As analytical ground truth is unavailable for the complex posteriors in `posteriordb`, we establish a computational “gold standard” by aggregating 100 independent MCMC and bridge sampling runs (totaling 400,000 posterior draws with low autocorrelation per model), which will serve as the proxy for the true marginal likelihood against which individual MCSE predictions are validated.

We begin by introducing a simple toy example, which serves to illustrate the conditions under which the bridge sampler performs effectively, as well as the circumstances in which it has too high variance to be useful. Following this, we present results using many real models and datasets sourced from the posterior database `posteriordb`, introduced by Magnusson et al. (2025).

6.1 Sparse Linear Regression with Increasing Number of Covariates

We begin by exploring the performance of bridge sampling within the context of linear regression with a highly non-normal posterior, and particularly focusing on how the method behaves as the number of covariates increases and the posterior gets higher dimensional and more non-normal.

The simulated data for this analysis were generated as follows. Given $n = 100$ observations, the design matrix \mathbf{X} was created with k covariates, where $k \in \{10, 11, 12, \dots, 103\}$. Each element of \mathbf{X} was drawn from a standard normal distribution and scaled by $\frac{1}{\sqrt{n \times k}}$:

$$\mathbf{X} = \frac{1}{\sqrt{n \times k}} \boldsymbol{\xi}, \quad \text{where } \boldsymbol{\xi} \sim \mathcal{N}(0, 1)^{n \times k}.$$

The regression coefficients $\boldsymbol{\beta}$ were sampled from a standard normal distribution, with the last coefficient set to zero:

$$\boldsymbol{\beta} = (\beta_1, \beta_2, \dots, \beta_{k-1}, 0)^\top, \quad \text{where } \beta_i \sim \mathcal{N}(0, 1).$$

The response variable \mathbf{y} was generated as a linear combination of the covariates with added normal noise:

$$\mathbf{y} = \mathbf{X}\boldsymbol{\beta} + \frac{1}{\sqrt{n}} \boldsymbol{\epsilon}, \quad \text{where } \boldsymbol{\epsilon} \sim \mathcal{N}(0, 2).$$

The model is

$$\mathbf{y} = \mathbf{X}\boldsymbol{\beta} + \boldsymbol{\epsilon}, \quad \boldsymbol{\epsilon} \sim \mathcal{N}(0, \sigma^2 \mathbf{I}).$$

To induce a non-normal posterior, a regularized horseshoe prior $\text{RHS}(\tau, \lambda_i)$ (Pironen and Vehtari, 2017) was used for the regression coefficients $\boldsymbol{\beta}$. The RHS prior was implemented as a scale mixture of normals:

$$\beta_i \sim \mathcal{N}(0, \tau^2 \lambda_i^2), \quad \lambda_i \sim \text{Cauchy}^+(0, 1), \quad \tau \sim \text{Cauchy}^+(0, 1).$$

This mismatch between the data generation (Normal) and the estimation model (RHS) is intentional; it creates a challenging, funnel-like posterior geometry for the bridge sampler to integrate.

The posterior sampling was done using the `rstanarm` function `stan_glm` (Goodrich et al., 2024). Bridge sampling was done using `bridge_sampler` function in the `bridgesampling` package (Gronau et al., 2020a). We sampled 4000 posterior draws from each posterior, which is the default in `rstanarm`.

Figure 2 shows the standard deviations of log marginal likelihood and marginal likelihood estimates, and the MCSE estimate for the first. As the number of covariates increases, the posterior gets more high-dimensional and non-normal, increasing the variability of the bridge sampling estimates of the (log)

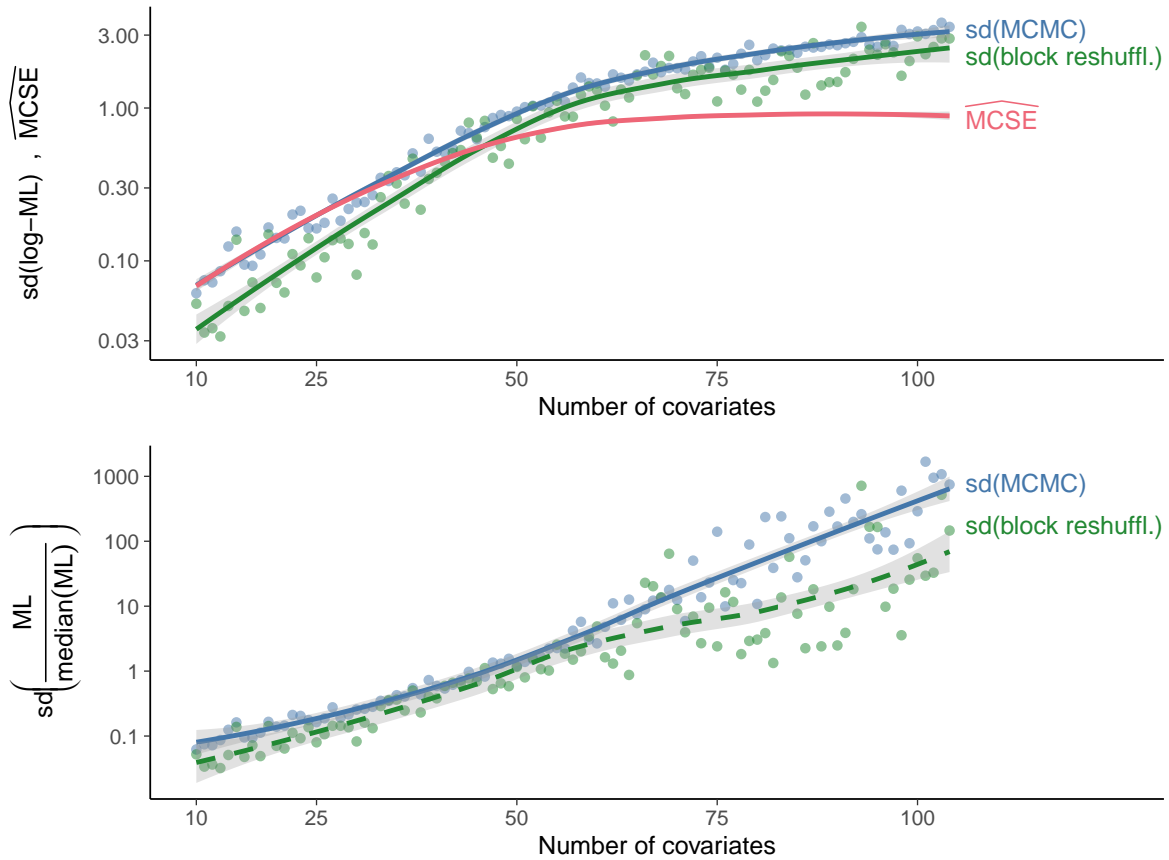


Figure 2. Top plot shows the standard deviation of the log marginal likelihood estimate (in log scale) from repeated running of MCMC and bridge sampling (solid line), the standard deviation of log marginal likelihood estimate from repeated running of bridge sampling with block reshuffling (long dashed line), and the MCSE estimate from a single bridge sampling estimate (dashed line). The bottom plot shows the standard deviation (normalized by the median marginal likelihood given the number of covariates) of the marginal likelihood estimate (in log scale) from repeated running of MCMC and bridge sampling (solid line) and the standard deviation of the log marginal likelihood estimate from repeated running of bridge sampling with block reshuffling (long dashed line).

marginal likelihood, with the analytic MCSE estimate starting to lose precision around 50 covariates. Consistent with our discussion in Section 5, the block reshuffling diagnostic slightly underestimates the total standard deviation in the highest dimensions due to the reuse of draws, yet correctly identifies the regime of instability. Furthermore, the correspondence between the standard deviation for the log marginal likelihood and the standard deviation for the marginal likelihood is very close to the correspondence between the standard deviations of normal and log normal distributions.

To give some idea of the scale of the potential error, we can consider using the (log) marginal likelihood for model comparison. Based on the experiments, the uncertainty in the log marginal likelihood estimates is quite well approximated by a normal distribution. With bridge sampling, the log marginal likelihood estimates for two models are independent, and if the MCSE are similar, then MCSE for difference of log marginal likelihoods is $\sqrt{2}$ times as big. If the true difference were 0, then a log marginal likelihood MCSE of about 0.5 would lead to 6% of the repeated estimates to be smaller than $1/3$ and 6% to be bigger

than 3, corresponding to moderate evidence for either model solely due to Monte Carlo variability. Thus, a desirable MCSE for the log marginal likelihood would be less than 0.2 if the difference is expected to be small. Naturally, this depends on the specific use case.

If using Stan for the posterior inference, we recommend starting with the default number of posterior draws (4000), and then adjusting based on the observed MCSE. For simple cases, MCSE with the default number of draws may already be sufficient (at the time of writing, the `bridgesampling` package documentation states “The computation of marginal likelihoods based on bridge sampling requires a lot more posterior draws than usual. A good conservative rule of thumb is perhaps 10-fold more draws”). If the estimated MCSE is too high, more posterior draws can be obtained. As the variance of the estimator is finite, we may assume in many cases that MCSE halves by quadrupling the number of posterior draws (based on CLT) and use that rule to estimate how many posterior draws are required for the desired precision. If the bound for either numerator or denominator in the bridge sampling equation is far, then even more draws may be required for the desired precision (Vehtari et al., 2024).

In this example the biggest standard deviation for the log marginal likelihood is 2.5, which in comparing models with no true difference would lead to 10% of the repeated estimates to be smaller than 1/100 and 10% to be bigger than 100, corresponding to extreme evidence for either model depending on the specific realization of the Monte Carlo draws. To get a MCSE of 2.5 reduced to around 0.2 would require at least 156 times more posterior draws, that is, more than 600 000 posterior draws (and might require more if the pre-asymptotic convergence rate is lower due to a long tail and very large bound). Alternate proposal distributions may also improve the performance.

We next look at the use of the Pareto- \hat{k} as a further diagnostic. Figure 3 shows the average Pareto- \hat{k} diagnostic using the default number of the tail values (135 given 2000 draws, continuous lines). Pareto- \hat{k} 's for both numerator and denominator are below 0.5 when the number of covariates is less than 21, and thus, in those cases, we could trust MCSE estimates. However, Figure 2 did show that the MCSE estimate was precise up to about 50 covariates. In this case, the tails of the numerator and denominator distributions are far from Pareto shape, and Pareto- \hat{k} with the default number of tail values gives too high values. Figure 3 also shows the average Pareto- \hat{k} diagnostic using only 10 tail values (dashed lines). Now Pareto- \hat{k} s for both numerator and denominator are below 0.5 when the number of covariates is less than 42, which better matches the range when the MCSE estimate starts to fail. This confirms that even though the distributions are theoretically bounded, in the pre-asymptotic regime the finite-sample draws exhibit heavy-tailed behavior indistinguishable from unbounded distributions, rendering the variance-based MCSE unreliable. In this case, the average Pareto- \hat{k} diagnostic using only 10 tail values matches the average behavior, but for a single case the Pareto- \hat{k} using only 10 tail values has too big variability to be a practical diagnostic. We leave it for future research to develop an alternative tail shape diagnostic that would work well for such bounded distributions that arise in bridge sampling.

6.2 `posteriordb` Posteriors

To gain further insights into the performance of bridge sampling under different conditions, we proceed to an examination of 41 models and posteriors from the `posteriordb` database (Magnusson et al., 2025) plus a multi-component Gaussian process model of birthday data (Zhang et al., 2022). The posterior distributions selected for this study are the same as those analyzed by Zhang et al. (2022) plus several additional high-dimensional posteriors that have been included in `posteriordb` more recently. They include a representative set of real-life posteriors with varying dimensionality, non-normality, funnelness, and multi-modality. The list of posteriors, the number of posterior dimensions (in unconstrained space), and a short description of the model are provided in Appendix A. For many models the Stan code used is dropping the constant terms, so the estimated marginal likelihoods are also missing that constant, but

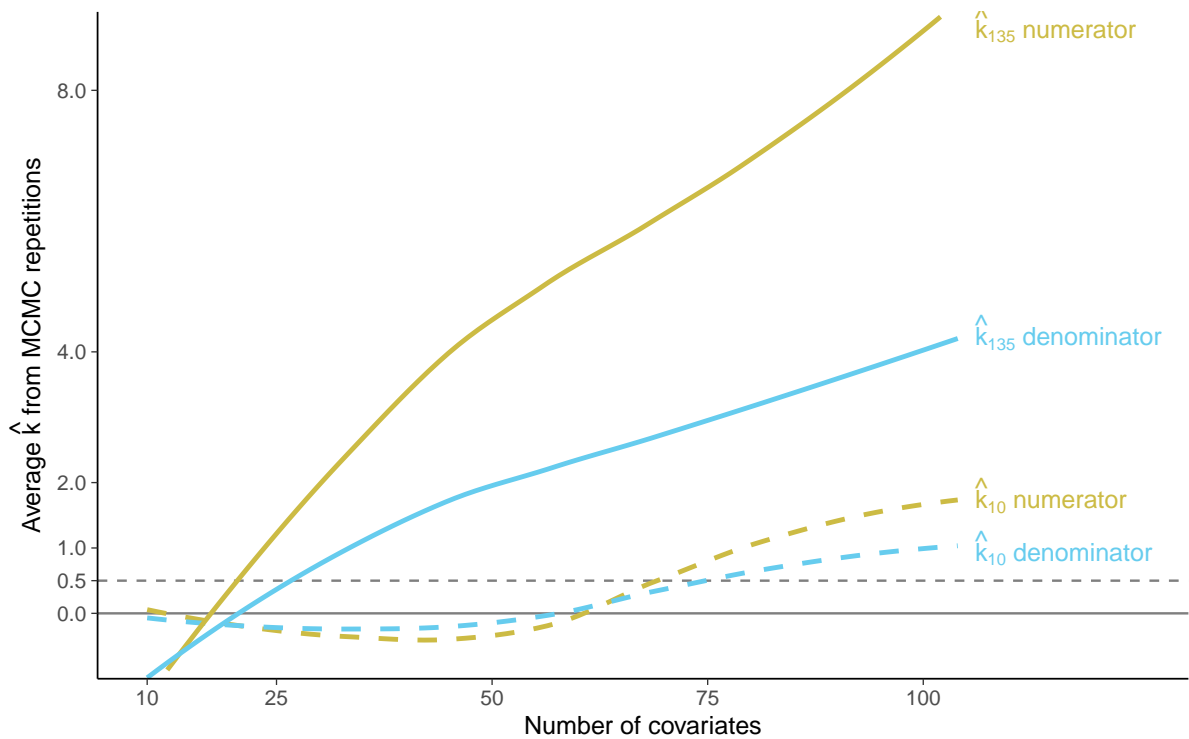


Figure 3. Pareto- \hat{k} diagnostic in the linear regression example with the increasing number of covariates for the distribution of terms in the numerator and denominator (as labeled in the plot). The plot shows the average over 100 independent MCMC runs of estimated \hat{k} using the default number of tail draws (135) and only 10 tail draws with continuous and long dashed lines, respectively.

that does not affect the estimation variability. We sampled 4000 posterior draws from each posterior using `CmdStanR` with the default options except using the Pathfinder algorithm (Zhang et al., 2022) to initialize MCMC for improved convergence speed and reliability. We did check that the MCMC sampling performed reasonably for all posteriors, but in some cases there are divergences which indicate the possibility of biased estimates, which can also increase the bias and variability in the (log) marginal likelihood estimates. We did not compute true marginal likelihood for any of the posteriors, and it would be impossible for most of the posteriors, but compare the performance to the average over 100 independent repeated runs. To quantify the computational gain, for one of the most complex models in our set (Birthdays GP), these 100 independent MCMC runs took 1571.4 minutes, whereas generating 100 estimates via block reshuffling took only 72.8 minutes (a $\approx 21.5\times$ speedup).

Figures 4 and 5 show MCSE and standard deviation of log marginal likelihood estimates from block reshuffling vs standard deviation of log marginal likelihood estimates from repeated MCMC runs. MCSE estimates are quite precise for most of the posteriors while block reshuffling standard deviation tends to be slightly smaller than the MCMC standard deviation when the true standard deviation is also small. For 36/42 posteriors MCSE and MCMC standard deviation are below 0.2. For the Birthdays posterior we can estimate that 13 times more posterior draws, that is, at least 52 000 posterior draws would be required to get a MCSE of 0.2 or smaller. For the Presidential votes hierarchical Gaussian process posterior we can estimate that 500 times more posterior draws, that is, at least 2 million posterior draws would be required to get MCSE of 0.2 or smaller, which starts to be an impractically large number of draws.

Figure 6 shows the strong dependency between the number of posterior dimensions and standard deviation of log marginal likelihood estimates. The increasing number of dimensions increases the variability, but only posteriors with more than 300 dimensions have standard deviation larger than 0.2, which can be considered to be an excellent result. The variation within the posteriors having the same dimensionality can be explained by a) how different the posterior is from normal, and b) how efficient MCMC sampling is. For example, eight schools with centered parameterization is known to have a strong funnel-shaped posterior which Stan’s current MCMC algorithm is not able to sample efficiently.

7 Discussion

Our primary contribution is a diagnostic framework designed to quantify uncertainty at three distinct levels.

First, we derived and validated a closed-form Monte Carlo standard error (MCSE) for the bridge sampling estimator. While the asymptotic properties of bridge sampling are well-established (Meng and Wong, 1996; Frühwirth-Schnatter, 2004), practical reporting of uncertainty has been inconsistent. By verifying the MCSE against extensive empirical benchmarks from `posteriorsdb`, we demonstrate that for a range of posteriors, the standard delta-method approximation is sufficiently precise. This provides practitioners with a computationally cheap baseline diagnostic that should be standard reporting practice, akin to effective sample size (ESS) for MCMC.

Second, we bridged the gap between the theoretical boundedness of the estimator and its finite-sample behavior. While Meng and Wong (1996) showed that the optimal bridge function yields bounded ratios, we identified a “pre-asymptotic regime” where these bounds are irrelevant for realistic sample sizes. By adapting the Pareto- k diagnostic from importance sampling (Vehtari et al., 2024), we provide a method to detect when the estimator is dominated by rare events, extending the utility of tail-index diagnostics beyond unbounded importance sampling to the bounded (but heavy-tailed in behavior) setting of bridge sampling.

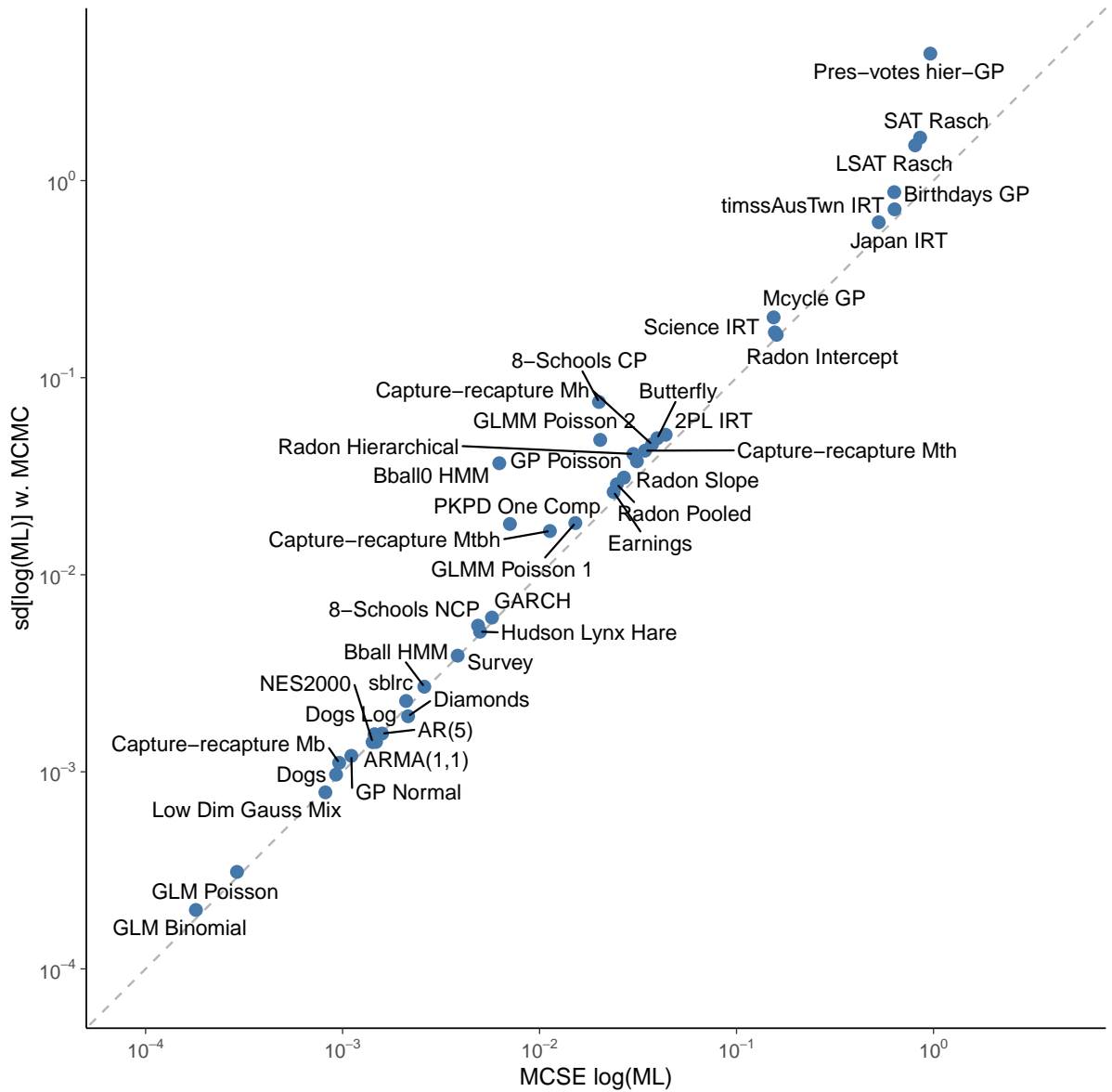


Figure 4. posterior db posteriors + Birthdays: Estimated MCSE vs standard deviation of log marginal likelihood estimates from repeated MCMC runs. MCSE estimate has small bias except for a few posteriors with the highest variability.

Bridge Sampling Diagnostics

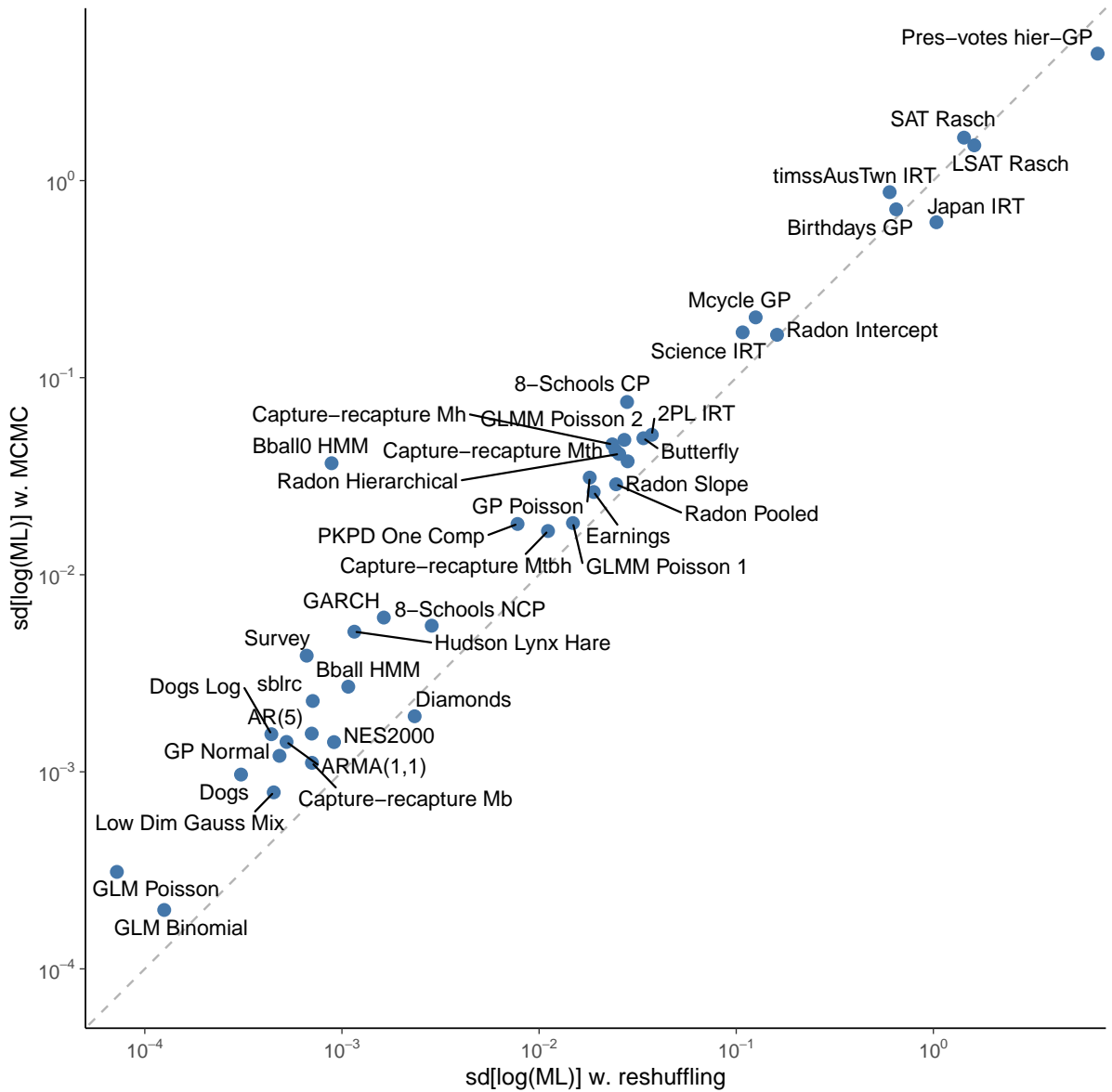


Figure 5. posteriordb posteriors + Birthdays: Standard deviation of log marginal likelihood estimates from block reshuffling vs standard deviation of log marginal likelihood estimates from 100 repeated MCMC runs. Block reshuffling underestimates the small variability estimates, but has small bias in case of high variability.

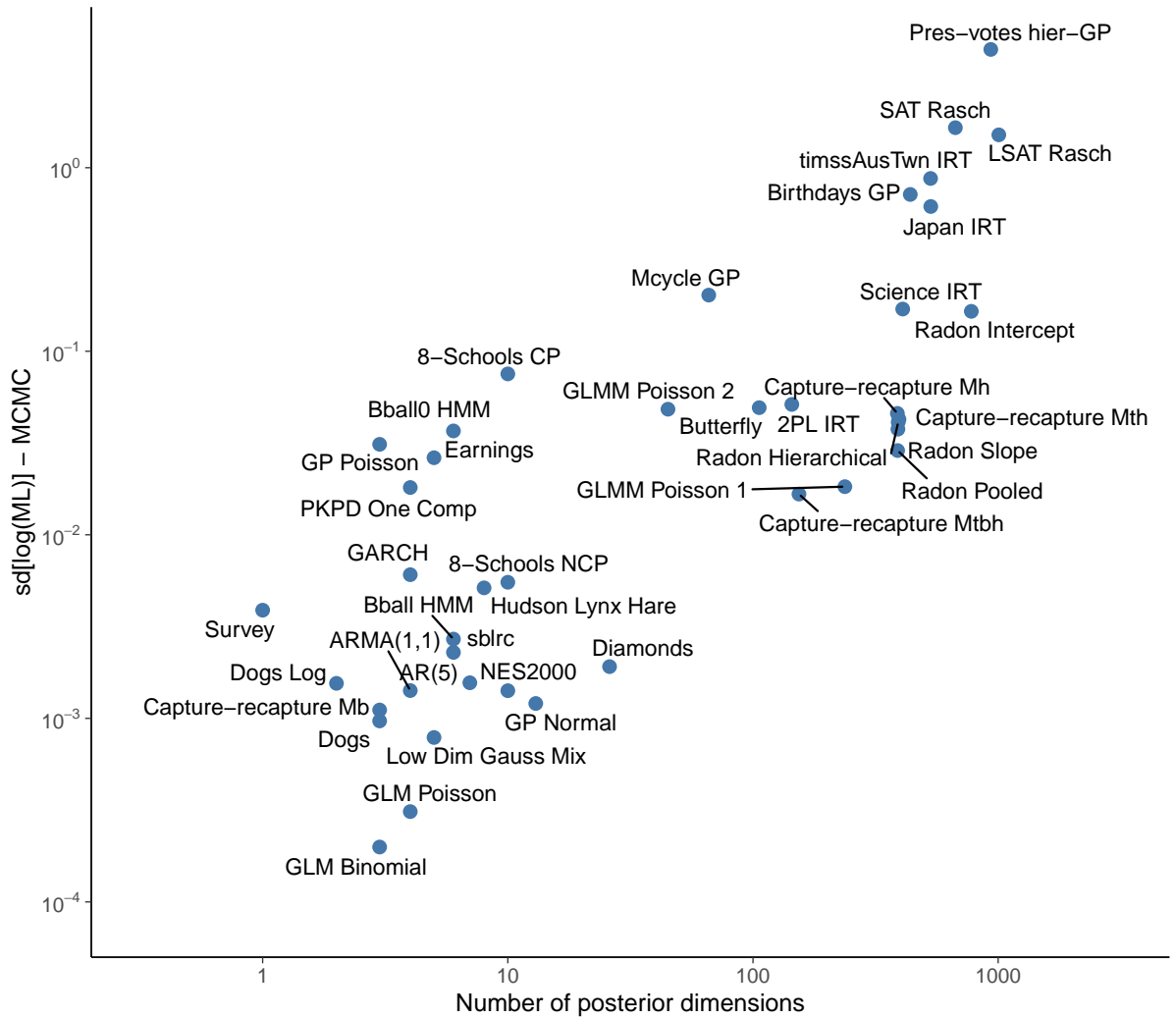


Figure 6. posteriors + Birthdays: The number of posterior dimensions vs standard deviation of log marginal likelihood estimates from repeated MCMC runs. The estimate variability tends to increase with the number of dimensions, which is natural due to the curse of dimensionality. In addition, there is variation depending on how non-normal the posterior distribution is.

Third, we introduced block reshuffling as a bootstrapping-based diagnostic, allowing practitioners to assess the shape and skewness of the estimator’s sampling distribution without relying on the normality assumptions inherent in the standard analytic MCSE. While it may underestimate total variance due to sample reuse, it provides a critical check for non-normality and instability in finite samples.

We recommend a stepwise workflow: start with the analytic MCSE; if $\hat{k} > 0.5$ or if high precision is critical, verify stability with block reshuffling. This approach moves marginal likelihood estimation from a “black box” procedure to a transparent, diagnosable component of the Bayesian workflow.

8 Acknowledgments

We thank Ozan Adıgüzel for making some of the initial experiments (not shown in this paper), and Noa Kallioinen and Anna Riha for helpful comments and feedback. We also acknowledge the computational resources provided by the Aalto Science-IT project.

9 Funding

We acknowledge the support by the Research Council of Finland Flagship programme: Finnish Center for Artificial Intelligence, Research Council of Finland project (340721), and The Aalto Science Institute international summer research internship programme, as well as the computational resources provided by the Aalto Science-IT project.

10 Data Availability Statement

The data and code that support the findings of this study are available at the following URL: https://github.com/GiorgioMB/bridgesampling_paper_code. Monte Carlo standard error computation is also included in `bridgesampling` package <https://github.com/quentingronau/bridgesampling/>.

References

- Bennett, C. H. (1976). Efficient estimation of free energy differences from Monte Carlo data. *Journal of Computational Physics*, 22(2):245–268.
- Fourment, M., Magee, A. F., Whidden, C., Bilge, A., Matsen, Frederick A, I., and Minin, V. N. (2019). 19 dubious ways to compute the marginal likelihood of a phylogenetic tree topology. *Systematic Biology*, 69(2):209–220.
- Friel, N. and Wyse, J. (2012). Estimating the evidence – a review. *Statistica Neerlandica*, 66(3):288–308.
- Frühwirth-Schnatter, S. (2004). Estimating marginal likelihoods for mixture and Markov switching models using bridge sampling techniques. *The Econometrics Journal*, 7(1):143–167.
- Gelman, A. and Meng, X.-L. (1998). Simulating normalizing constants: from importance sampling to bridge sampling to path sampling. *Statistical Science*, 13(2):163 – 185.
- Gelman, A. and Rubin, D. B. (1992). Inference from Iterative Simulation Using Multiple Sequences. *Statistical Science*, 7(4):457 – 472.

- Goodrich, B., Gabry, J., Ali, I., and Brilleman, S. (2024). rstanarm: Bayesian applied regression modeling via Stan. R package version 2.32.1.
- Gronau, Q., Singmann, H., and Wagenmakers, E.-J. (2020a). bridgesampling: An R Package for Estimating Normalizing Constants. *Journal of Statistical Software*, 92(10).
- Gronau, Q. F., Heathcote, A., and Matzke, D. (2020b). Computing bayes factors for evidence-accumulation models using warp-iii bridge sampling. *Behavior Research Methods*, 52(2):918–937.
- Gronau, Q. F., Sarafoglou, A., Matzke, D., Ly, A., Boehm, U., Marsman, M., Leslie, D. S., Forster, J. J., Wagenmakers, E.-J., and Steingroever, H. (2017). A tutorial on bridge sampling. *Journal of Mathematical Psychology*, 81:80–97.
- Hall, P. (1992). *The Bootstrap and Edgeworth Expansion*. Springer-Verlag, New York.
- Kunsch, H. R. (1989). The Jackknife and the Bootstrap for General Stationary Observations. *The Annals of Statistics*, 17(3):1217 – 1241.
- Liu, R. Y. and Singh, K. (1992). Moving blocks jackknife and bootstrap capture weak dependence. In *Exploring the Limits of Bootstrap*, pages 225–248. Wiley.
- Magnusson, M., Torgander, J., Bürkner, P.-C., Zhang, L., Carpenter, B., and Vehtari, A. (2025). posteriordb: Testing, benchmarking and developing Bayesian inference algorithms. In Li, Y., Mandt, S., Agrawal, S., and Khan, E., editors, *Proceedings of The 28th International Conference on Artificial Intelligence and Statistics*, volume 258 of *Proceedings of Machine Learning Research*, pages 1198–1206. PMLR.
- Meng, X.-L. and Schilling, S. (2002). Warp bridge sampling. *Journal of Computational and Graphical Statistics*, 11(3):552–586.
- Meng, X.-L. and Wong, W. H. (1996). Simulating Ratios of Normalizing Constants Via a Simple Identity: A Theoretical Exploration. *Statistica Sinica*, 6(4):831–860. Publisher: Institute of Statistical Science, Academia Sinica.
- Overstall, A. M. and Forster, J. J. (2010). Default bayesian model determination methods for generalised linear mixed models. *Computational Statistics & Data Analysis*, 54(12):3269–3288.
- Piironen, J. and Vehtari, A. (2017). Sparsity information and regularization in the horseshoe and other shrinkage priors. *Electronic Journal of Statistics*, 11:5018–5051.
- Vehtari, A., Gelman, A., Simpson, D., Carpenter, B., and Bürkner, P. C. (2021). Rank-normalization, folding, and localization: An improved \hat{R} for assessing convergence of MCMC. *Bayesian Analysis*, 16:667–718.
- Vehtari, A., Simpson, D., Gelman, A., Yao, Y., and Gabry, J. (2024). Pareto Smoothed Importance Sampling. *Journal of Machine Learning Research*, 25(72):1–58.
- Wang, L., Jones, D. E., and Meng, X.-L. (2022). Warp bridge sampling: The next generation. *Journal of the American Statistical Association*, 117(538):835–851.
- Wong, J. S. T., Forster, J. J., and Smith, P. W. F. (2020). Properties of the bridge sampler with a focus on splitting the mcmc sample. *Statistics and Computing*, 30(4):799–816.
- Zhang, L., Carpenter, B., Gelman, A., and Vehtari, A. (2022). Pathfinder: Parallel quasi-Newton variational inference. *Journal of Machine Learning Research*, 23(306):1–49.

A posteriordb Posteriors and Birthdays Posterior

We used 41 posteriors from posteriordb and a multi-component Gaussian process model (gpb6), which was used by Zhang et al. (2022). Table A.1 lists the posteriordb IDs, the posterior names used in the figures in this paper, the number of posterior dimensions (in unconstrained space), and a short description of the model.

Table A.1. Posteriors from posteriordb used in Section 6. Columns: posteriordb ID, name used in the plots, number of unconstrained posterior dimensions D and a brief description.

posteriordb id	plot names	D	description
arK-arK	AR(5)	7	AR-5 model
arma-arma11	ARMA(1,1)	4	ARMA
bball_drive_event_1-hmm_drive_1	Bball HMM	6	Hidden Markov model
bball_drive_event_0-hmm_drive_0	Bball0 HMM	6	Hidden Markov model
-	Birthdays GP	438	Multi-component GP time series model (gpb6)
butterfly-multi_occupancy	Butterfly	106	Multiple Species-site occupancy model
diamonds-diamonds	Diamonds	26	Multiple highly correlated predictors log-log model
dogs-dogs	Dogs	3	Logistic mixed effects model
dogs-dogs_log	Dogs Log	2	Logarithmic mixed effects model
earnings-logearn_interaction	Earnings	5	Multiple predictors interacting log-linear model
eight_schools-eight_schools_centered	8-Schools CP	10	A centered hierarchical model for 8 schools
eight_schools-eight_schools_noncentered	8-Schools NCP	10	A non-centered hierarchical model for 8 schools
garch-garch11	GARCH	4	Generalized autoregressive conditional heteroscedastic model
GLM_Binomial_data-GLM_Binomial_model	GLM Binomial	3	Success rate of peregrine broods
GLM_Poisson_Data-GLM_Poisson_model	GLM Poisson	4	Poisson GLM for modeling a population of peregrines
GLMM_data-GLMM1_model	GLMM Poisson 1	237	GLMM for peregrine population size
GLMM_Poisson_data-GLMM_Poisson_model	GLMM Poisson 2	45	GLMM for peregrine population size with random site and year effects
gp_pois_regr-gp_regr	GP Normal	3	Gaussian process regression
gp_pois_regr-gp_pois_regr	GP Poisson	13	Gaussian process Poisson regression
hmm_example-hmm_example	HMM	4	Hidden Markov model
hudson_lynx_hare-lotka_volterra	Hudson Lynx Hare	8	Lotka-Volterra Model
irt_2pl-irt_2pl	2PL IRT	144	Two-parameter logistic item response theory model
fims_Aus_Jpn_irt-2pl_latent_reg_irt	Japan IRT	531	Two-parameter logistic item response theory model
low_dim_gauss_mix-low_dim_gauss_mix	Low Dim Gauss Mix	5	A Two-dimensional Gaussian mixture model
lsat_data-lsat_model	LSAT Rasch	1006	Random effects (Rasch) model for true difficulty of LSAT questions
Mb_data-Mb_model	Capture-recapture Mb	3	Inferring population size considering immediate trap-response
mcycle_gp-accel_gp	Mcycle GP	66	Heteroscedastic Gaussian processes
Mh_data-Mh_model	Capture-recapture Mh	388	Logistic-normal heterogeneity model
Mtbh_data-Mtbh_model	Capture-recapture Mtbh	154	Capture-recapture model where detection probability varies by occasion

Micaletto and Vehtari

posteriordb id	plot names	D	description
Mth_data-Mth_model	Capture-recapture Mth	394	Capture-recapture model where detection probability varies by occasion and heterogeneity
nes2000-nes	NES2000	10	Multiple predictor linear model
one_comp_mm_elim_abs- one_comp_mm_elim_abs	PKPD One Comp	4	One compartment PKPD model
radon_all- radon_hierarchical_intercept _noncentered	Radon Hierarchical	391	A county intercept and county level covariate for Radon data (non-centered)
radon_all- radon_variable_intercept_ _slope_noncentered	Radon Intercept	777	Variable intercept and slope hierarchical for Radon data (noncentered)
radon_all- radon_partially_pooled_ _noncentered	Radon Pooled	389	Hierarchical intercept model for Radon data (non-centered)
radon_all- radon_variable_slope_ _noncentered	Radon Slope	390	Variable slope hierarchical for Radon data (non-centered)
sat-hier_2pl	SAT Rasch	670	Hierarchical two-parameter logistic item response model
sblrc-blr	sblrc	6	A Bayesian linear regression model with vague priors
science_irt-grsm_latent_reg_irt	Science IRT	408	Rating scale and generalized rating scale models with latent regression
state_wide_presidential_votes-hierarchical_gp Survey_data-Survey_model	Pres-votes hier-GP Survey	933 1	Hierarchical Gaussian process Inferring the return rate and number of surveys from observed returns
timssAusTwn_irt-gpcm_latent _reg_irt	timssAusTwn IRT	530	Partial credit and generalized partial credit models with latent regression